Design and Optimization of Compressor Airfoils by Using Class Function / Shape Function Methodology

Daniel Giesecke[1], Udo Stark[2], Rubén Harms Garcia[1], Jens Friedrichs[1]

ISROMAC 2017

International Symposium on Transport Phenomena and Dynamics of Rotating Machinery

Hawaii, Maui

December 16-21, 2017

Abstract

This paper describes a new design method for high Reynolds number subsonic compressor blade sections for industrial gas turbines and compressors. The focus is on the middle and end stages, where the Reynolds numbers are about 2 to 6×10^6 and the Mach numbers between 0.4 and 0.8. The new design method combines i) a parametric geometry definition method, ii) a fast blade-to-blade flow solver, and iii) an optimization tool with a suitable objective function. The development of a new blade section is based on a conventional NACA-65 design, subsequently modified to an optimized CSM profile, where CSM means Class Function / Shape Function Methodology.

The new profile shapes are obtained by superimposing a camber line and a thickness distribution. Both the camber line and the thickness distribution are prescribed as analytical functions to cut down the CPU-time for geometry set up and to guarantee smooth geometries. Numerical calculations are performed by applying the two-dimensional blade-to-blade solver MISES. The optimization method used in this paper is the single-objective genetic algorithm (SOGA) from the DAKOTA library. The objective function consists of 5 components and takes into account the whole loss polar. The corresponding computing time is relatively short - that is 1 to 2 days.

At high Reynolds number, the new profiles show decreased design point losses and increased operating limits compared to corresponding results using conventional NACA-65 profiles. In addition, the present results show close agreement with those produced by so-called high performance profiles of the relevant literature.

Keywords

Compressor — Design — Optimization

[1]*Institute of Jet Propulsion and Turbomachinery, TU Braunschweig, Germany*

[2]*Institute of Fluid Mechanics, TU Braunschweig, Germany*

***Corresponding author**: d.giesecke@ifas.tu-braunschweig.de

INTRODUCTION

High Reynolds numbers and moderate subsonic Mach numbers are typical for the compressor middle and end stages of industrial gas turbines and compressors. The Reynolds numbers of the order of 2 to 6×10^6 [1] are much higher than the corresponding aeroengine numbers of about 0.6 to 1.2×10^6 [1]. When this was realized some twenty years ago, several new methods were developed taking into account the high Reynolds number and high turbulence effects on boundary layer transition [2, 3]. The new blade sections typically show a front loaded pressure distribution, a boundary layer transition (bypass transition) next to the pressure minimum at about 7 to 10% true chord, and a suction side deceleration whose gradient becomes increasingly lower towards the trailing edge. These features usually guarantee a successful design with low design-point losses and low off-design losses and extremely wide loss polars. However, the existing methods have generally long computing times of up to two weeks [3] for a complete loss polar. One of the reasons for this is probably the relative large number of geometric parameters (10 in [2] and 20 in [3]) which will all have to be optimized in a time-consuming optimization process. A new method, described in this paper, has only three geometric parameters that have to be optimized. This, together with an analytical formulation of the thickness distribution and camber line, leads to relatively short computing times of two days only. The paper concludes with the introduction and description of the two test cases - one of them a redesign of Profile No. 4 of the Design Case No. 4 in [2].

1. METHODS

The new design method combines i) a parametric geometry definition method, ii) a fast blade-to-blade flow solver, and iii) an optimisation tool with a suitable objective function. In the present work, the development of a new blade section is based on a conventional NACA-65 design subsequently modified to an optimized CSM profile, where CSM means Class Function / Shape Function Methodology [4]. The individual design steps may be summarized as follows: i) design of a conventional NACA-

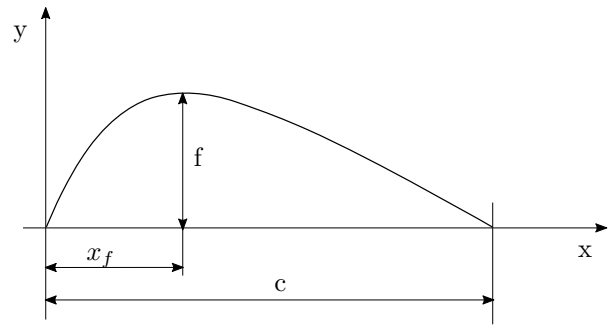

Figure 1. Camber line parameters

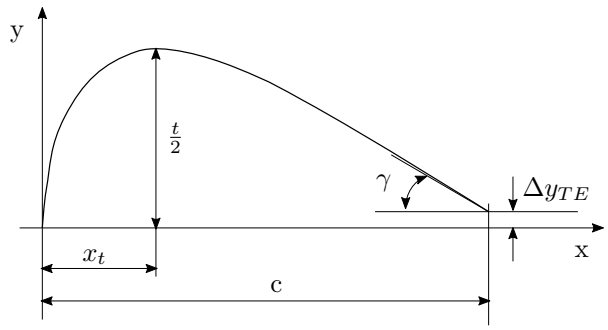

Figure 3. Thickness parameters

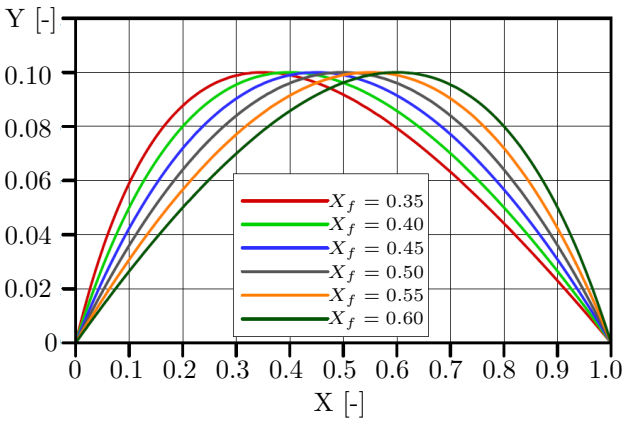

Figure 2. Camber lines of max. camber $f/c = 0.1$ at various chordwise positions

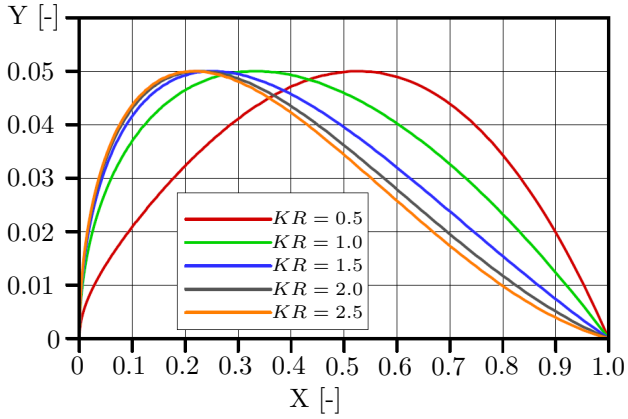

Figure 4. Thickness distributions of max. thickness $t/c = 0.1$ at various chordwise positions $X_t(KR)$

65 profile for a prescribed set of design parameters, ii) design of a CSM reference profile based on modified parameters of the conventional NACA-65 profile, and iii) search of an optimized CSM profile.

1.1 Blade Section Geometry

The challenge for the geometry method is to produce a fast analytical procedure with a small number of parameters for the design of subsonic, high Reynolds number compressor blade sections. The section shapes are obtained by superimposing a camber line and a thickness distribution. Both the camber line and the thickness distributions are prescribed by analytical functions to cut down the CPU-time for geometry set up and to guarantee smooth geometries.

The camber lines are so-called generalized parabolic arc lines [5] of the form

$$Y_c(X) = a \cdot \frac{X(1-X)}{1+bX} \tag{1}$$

with a and b representing the following abbreviations

$$a = \frac{1}{X_f^2}\frac{f}{c} \qquad \text{and} \qquad b = \frac{1-2X_f}{X_f^2}$$

with parameters f/c as maximum ordinate (expressed as fraction of chord) and X_f as chordwise position of the maximum ordinate, see Fig. 1. As an example, Fig. 2 shows an evaluation of the above formula for $f/c = 0.1$ and various values of the chordwise position X_f of the maximum ordinate.

The thickness distributions, as seen in Fig. 3, are derived from the following formulas representing the Class Function / Shape Function Methodololgy [4] in its simplest form (scaling factor omitted).

$$Y_t(X) = C(X) \cdot S(X) + X \cdot \Delta Y_{TE}. \tag{2}$$

with Class Function

$$C(X) = \sqrt{X} \cdot (1-X) \tag{3}$$

and Shape Function

$$S(X) = KR \cdot (1-X) + \frac{1}{KR} \cdot X, \tag{4}$$

where KR is a shape parameter determining the leading edge radius R_{LE}

$$S\,(0) = \sqrt{2R_{LE}}, \tag{5}$$

the trailing edge angle γ

$$S(1) = tan\gamma + \Delta Y_{TE} \tag{6}$$

and the maximum thickness location X_t

$$Y_t'(X_t) = \sqrt{(X_t)} \cdot (1 - X_t) \cdot S'(X_t) \tag{7}$$

$$+ \left[-\sqrt{(X_t)} + \frac{1 - X_t}{2\sqrt{X_t}} \right] \cdot S(X_t) + \Delta Y_{TE} \tag{8}$$

$$= 0. \tag{9}$$

As an example, Fig. 4 shows an evaluation of the above formulas for $t/c = 0.1$, $\Delta Y_{TE} = 0$ and various values of the shape parameter KR.

Altogether, the geometry model has finally only three parameters: two for the camber line and one for the thickness distribution for each blade design.

1.2 Blade-to-Blade Flow Solver

The blade-to-blade flow solver MISES 2.63 [6] has been selected as the flow code for the optimization. This code describes the inviscid flow using the steady Euler equations [7], while the viscous effects are modeled by the integral boundary layer equations [8]. The coupled system of nonlinear equations is solved by a Newton technique. The boundary conditions are defined by those of the cascade to be designed and optimized. The design inlet Mach number is kept constant while the inlet angle is varied between positive and negative stall. Boundary layer transition is predicted using the criterion of Abu-Ghannam / Shaw [9] in a slightly modified version [10] to achieve a better modeling of the flow physics at transition. The solver has been sufficiently validated for cascade flows at low and high Reynolds numbers, [11, 12] and [2, 13] respectively, and at various turbulence levels with and without turbulence grids [1]. AVDR effects are taken into account by a hyperbolic tangent variation of the streamtube thickness [14, 15].

1.3 Optimization Method

The optimization method used in this paper is the single-objective genetic algorithm (SOGA) from the DAKOTA library [16]. The SOGA starts with a random generation of profiles within the limits of the geometric parameters (50 samples per generation). The generated individuals will be evaluated by means of an objective function and passed or not passed to the next generation (up to 19). The accepted individuals will be promoted, the others will be killed. The latter fail to produce the required exit angle β_2 in specific limits.

The objective function of the present investigation consists of 5 components and takes into account the whole loss characteristic. This function has previously been used by Köller et al. [2], by Sieverding et al. [3]

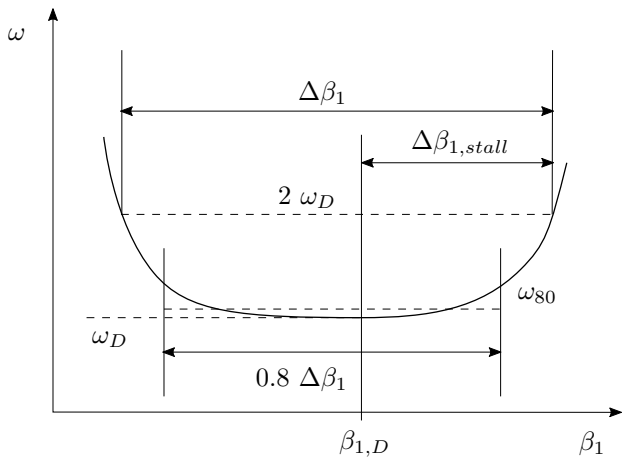

Figure 5. Parameters of the objective function, adapted from [3]

and is defined as follows:

$$OBF = C_1 \left(\frac{\omega_D}{\omega_{D,ref}} \right) + C_2 \left(\frac{\Delta\beta_{1,ref}}{\Delta\beta_1} \right) + C_3 \left(\frac{\Delta\beta_{1,stall,ref}}{\Delta\beta_{1,stall}} \right) + C_4 \left(\frac{\omega_{80}}{\omega_{80,ref}} \right) + C_5 \left(\frac{\sigma_{80}}{\sigma_{80,ref}} \right) \tag{10}$$

Each component of the function has been normalized using a corresponding reference value (index ref) of a suitable reference profile. An illustration of all components is shown in Fig. 5, where ω_D is the design loss coefficient at the design inlet angle $\beta_{1,D}$. A loss coefficient of twice the value of ω_D defines the operating range $\Delta\beta_1$ on the loss characteristic. The difference between the (positive) stall point and the design point is generally known as stall margin $\Delta\beta_{1,stall}$ or safety against stall. For the inner 80 % of the operating range the average value ω_{80} and the standard deviation σ_{80} are introduced to achieve a loss characteristics as flat as possible. The coefficients C are so-called weighting factors by which the relative importance of a component can be changed. Any change has to be specified by the user and validated by test runs. The results of this paper have been produced with the following weighting factors: $C_1 = 1$, $C_{2,4,5} = 0.5$ and $C_3 = 2$.

2. RESULTS

2.1 Test Case 1

In the present work, the development of a new blade section starts with a conventional NACA-65 profile which is subsequently modified to an optimized CSM profile. This development is best documented in table form with four columns for the different stages of the evolution,

Table 1. Test Case 1

Design Specifications			NACA65			CSM ref.		CSM opt.
Ma_1	=	0.44	X_f	=	0.5	$\longrightarrow$	0.45	$\longrightarrow$ 0.554
Re_1	=	2.5×10^6	f/c	=	0.055 (C)	$\longrightarrow$	0.055 (P)	$\longrightarrow$ 0.0451 (P)
β_1	=	47°	X_t	=	0.4	$\longrightarrow$	0.2281	$\longrightarrow$ 0.2290
β_2	=	29°					$KR = 2.0$	$KR = 1.97$
t/c	=	0.093	λ	=	34.7°	$\longrightarrow$	34.2°	$\longrightarrow$ 34.2°
s/c	=	0.87						
ΔY_{TE}	=	0.005						
$AVDR$	=	0.99						
Tu_1	=	3 %						

C: Circular Arc P: Parabolic Arc

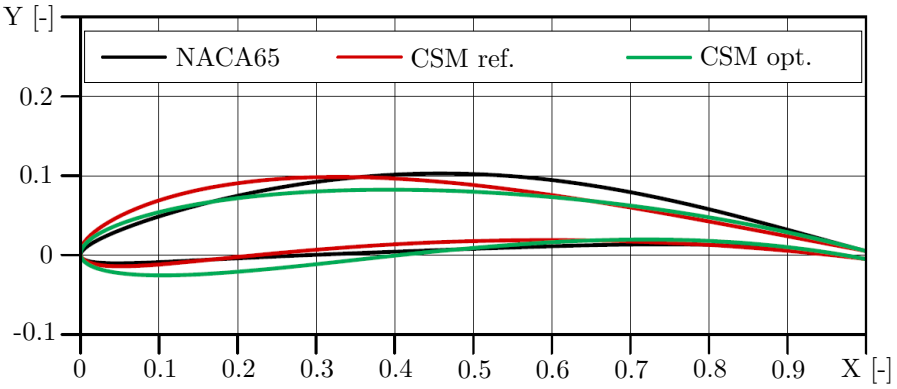

Figure 6. Test Case 1 profiles in comparison

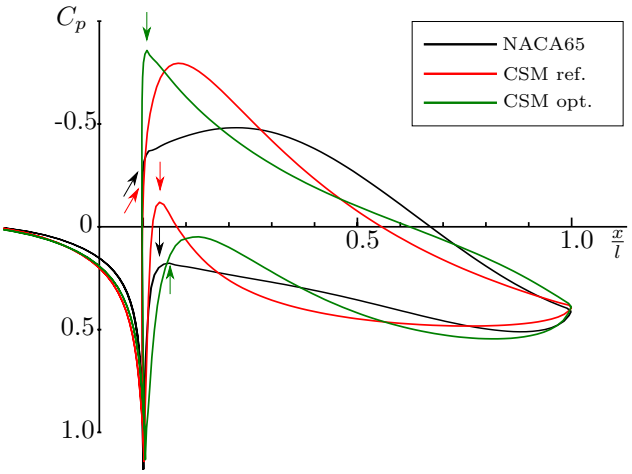

Figure 7. Test Case 1 pressure distributions at design inlet angle $\beta_1 = 47°$

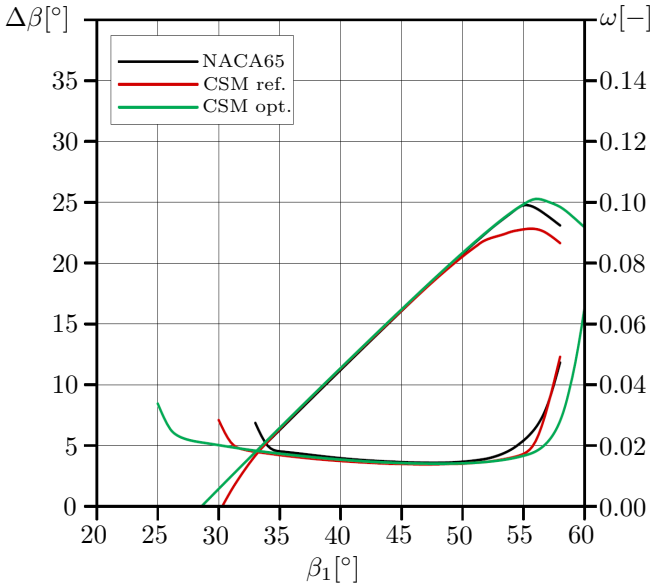

Figure 8. Test Case 1 overall performance characteristics

cf. Table 1 for Test Case 1. The first column lists the specifications for the new blade section to be designed. The following three columns present the main geometry parameters ($X_f, f/c$ and $X_f(KR)$) for the conventional NACA-65 profile in column 2, for the reference CSM profile in column 3 and for the optimized CSM profile in column 4. The estimated parameter values for the CSM profile are based on the corresponding values of the NACA-65 profile.

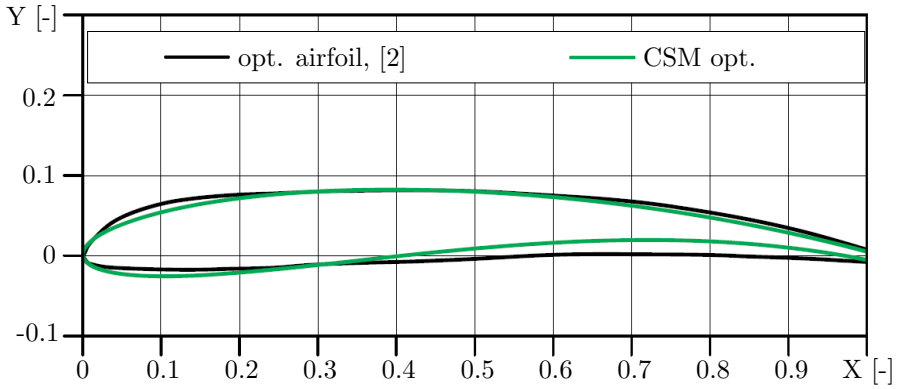

Figure 9. Optimized Test Case 1 profile in comparison with Test Case 4 profile of [2]

The new design method in this paper has been tested (Test Case 1) on the design of a high Reynolds number subsonic compressor blade section for industrial gas turbines and compressors. The design specifications belong to the Test Case 4 of reference [2], and are shown here in Table 1, first column. The Mach number, Reynolds number and turbulence level are $Ma_1 = 0.44, Re_1 = 2.5 \times 10^6$ and $Tu_1 = 3\%$ respectively. For further details see Table 1, columns 2, 3 and 4.

Figure 6 presents all three profiles - the conventional, the reference and the optimized profile. The corresponding blade pressure distributions are shown in Fig. 7 at design air inlet angle ($\beta_1 = 47°$). An inspection of the optimized pressure distribution led to the conclusion that optimization at high Reynolds numbers and turbulence levels of the present investigation inevitable ends up with a front loaded profile.

As indicated in Fig. 7, boundary layer transition (bypass transition) starts right after the leading edge on the suction side and somewhat downstream on the pressure side for both the conventional NACA-65 and the optimized CSM profile. Deceleration of the turbulent suction side boundary layer begins shortly after the leading edge for the optimized profile and at about 25% chord length for the conventional profile with a gradient becoming increasingly smaller or steeper respectively.

The controlled diffusion of the optimized CSM profile leads to a 0.8% reduction in design point losses. At off-design, the controlled diffusion concept remains essentially valid, specially at the higher inlet angles. There, the conventional profile is the first to reach the operational limit, while the optimized CSM profile generates a significantly increased operating range (+45%) and stall margin (+18%), cf. Fig. 8. The increase in operating range and stall margin is only partly due to decreasing deceleration gradients. The main cause turns out to be the reduced leading edge sharpness, which makes the profile less sensitive to off-design air inlet angles.

Figure 9 shows the optimized CSM profile of this paper together with the corresponding profile 4 of reference [2]. A comparison revealed noticeable differences, in particular close to the leading edge, where camber and curvature of the optimized CSM profile are relatively low. Numerical performance curves for both profiles are shown in Fig. 10, where they demonstrate a remarkable agreement in spite of considerably different profile shapes. In addition, Fig. 10 presents a comparison between numerical and experimental Test Case 4 results. The agreement, however, is not as good as before for the numerical results. These differences were already observed and described in [2], but a clear-cut explanation is still missing.

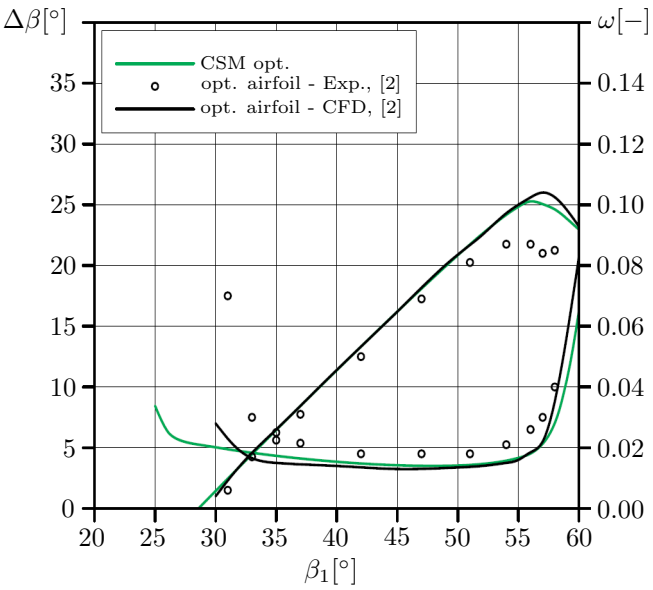

Figure 10. Optimized Test Case 1 performance in comparison with Test Case 4 profile of [2]

2.2 Test Case 2

The new design method of this paper has been developed for high Reynolds number applications. Nevertheless, it has been assumed that the new method might also be useful at lower Reynolds numbers (aeroengine Reynolds numbers or lower). This has been checked in

Table 2. Test Case 2

Design Specifications			NACA65				CSM ref.		CSM opt.
Ma_1	=	0.12	X_f	=	0.5	$\longrightarrow$	0.45	$\longrightarrow$	0.43
Re_1	=	3.5×10^5	f/c	=	0.1 (C)	$\longrightarrow$	0.1 (P)	$\longrightarrow$	0.1065 (P)
β_1	=	30°	X_t	=	0.4	$\longrightarrow$	0.2281	$\longrightarrow$	0.2128
β_2	=	0°					$KR = 2.0$		$KR = 2.84$
t/c	=	0.1	λ	=	13°	$\longrightarrow$	11.5°	$\longrightarrow$	11.5°
s/c	=	1.0							
ΔY_{TE}	=	0.005							
$AVDR$	=	1.0							
Tu_1	=	1 %							

C: Circular Arc P: Parabolic Arc

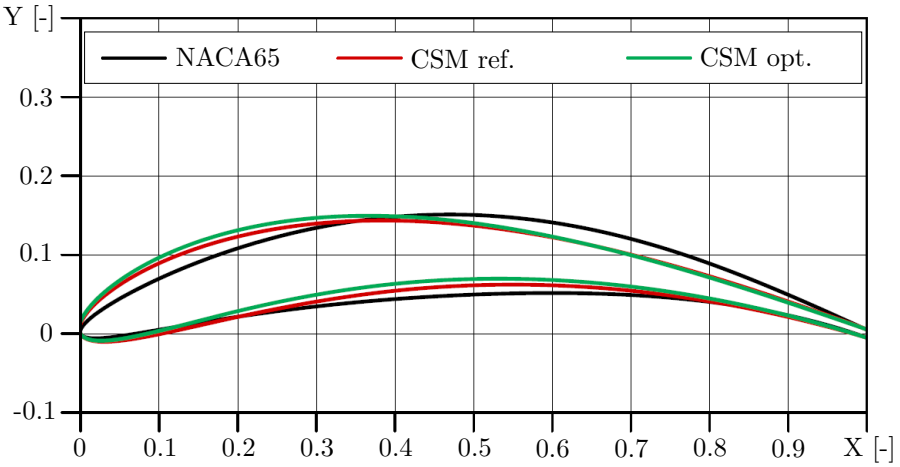

Figure 11. Test Case 2 profiles in comparison

a second test case, cf. Table 2 for Test Case 2. The design specifications appear in the first column, specially the Mach number $Ma_1 = 0.12$, the Reynolds number $Re_1 = 3.5 \times 10^5$ and the turbulence level $Tu_1 = 1\%$. The following three columns 2, 3 and 4 present, as before in Test Case 1, the main geometric parameters ($X_f, f/c$ and $X_f(KR)$) for the conventional NACA-65 profile, the reference CSM profile and the optimized CSM profile. All three profiles are shown in Fig. 11, the corresponding design point ($\beta_1 = 30°$) pressure distribution in Fig. 12 and the complete loss and turning characteristics in Fig. 13, together with experimental results for the NACA-65 profiles.

The most noticeable difference between the conventional NACA-65 and the optimized CSM profile is again the upstream moved location of the maximum thickness for the optimized CSM profile, cf. Fig. 11. Transition of the laminar boundary layer under Test Case 2 condition (low Reynolds number, low turbulence level) happens to occur via laminar separation bubbles downstream the pressure minimum on both sides of the profiles, cf. Fig. 12. In spite of a smaller deceleration gradient and a reduced leading edge sharpness, it is the optimized CSM profile that shows 13% higher design point losses compared to those for the conventional NACA-65 profile with relatively long portions of laminar boundary layers, cf. Fig. 13. However, thanks to the smaller deceleration gradient and the reduced leading edge sharpness, the predicted operating range and stall margin increased by more than 55 and 65% respectively.

3. CONCLUSION

In summary, a new method has been presented for the design of high Reynolds number, subsonic compressor blade sections for industrial gas turbines and compressors. By carefully selecting the number of design and optimization parameters, the combination with a genetic algorithm led to a competitive design method.

At high Reynolds numbers, the new profiles show decreased design point losses and increased operating limits compared to corresponding results using conventional NACA-65 profiles. In addition, the presented results show close agreement with those produced by so-called high performance profiles of the relevant literature. At low Reynolds numbers, the new profiles show slightly increased design point losses but again considerably in-

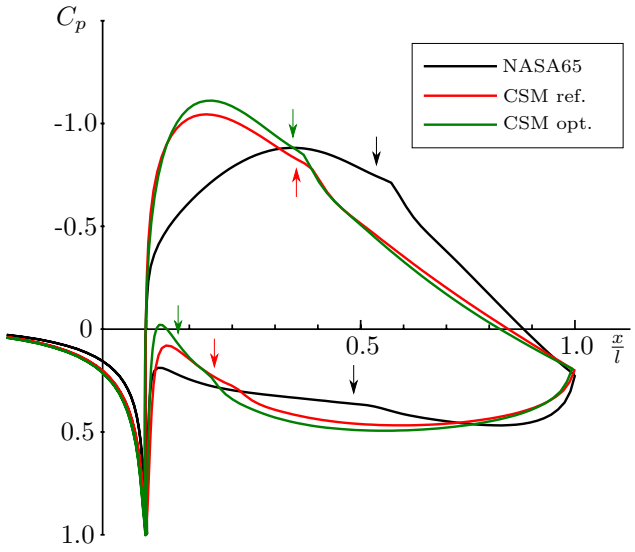

Figure 12. Test Case 2 pressure distributions at design inlet angle $\beta_1 = 30°$

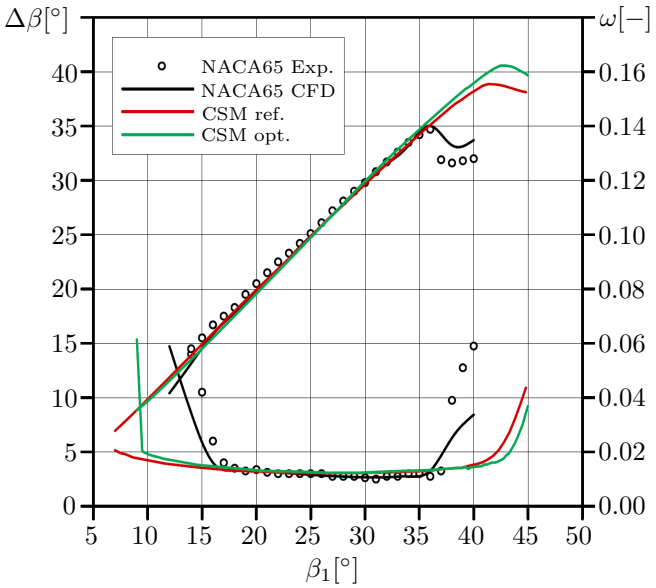

Figure 13. Test Case 2 overall performance characteristics

creased operation limits compared to conventional airfoil results.

However, for the chosen design approach further research is required. Applying it to airfoils for aeroengine application will be part of future research. Furthermore, cascade experiments would validate the new method and numerical results.

NOMENCLATURE

Symbols

a, b	parabolic mean arc line parameter
c	chord
C	Class Function
C_1 - C_5	weighting factors
f	maximum camber
KR	Shape Function factor
Ma	mach number
R_{LE}	leading edge radius
Re	Reynolds number
s	spacing
S	Shape Function
t	thickness
Tu	turbulence level
x_f	position of maximum camber
x_t	position of maximum thickness
X	dimensionless x value
X_f	dimensionless position of maximum camber
X_t	dimensionless position of maximum thickness
Y	dimensionless y value
Y_c	dimensionless y value for camber line
Y_t	dimensionless y value for thickness distribution
β	flow angle
$\Delta\beta_1$	operating range
Δy_{TE}	trailing edge thickness
ΔY_{TE}	dimensionless trailing edge thickness
γ	trailing edge angle
λ	stagger angle
ω	total pressure loss
σ	standard deviation

Subscripts

ref	reference
$stall$	stall margin
D	design
1	inlet
2	outlet
80	80 % of operating range

Abbreviations

AVDR	axial velocity density ratio
CPU	central processing unit
CSM	Class Function / Shape Function methodology
NACA	National Advisory Committee for Aeronautics
OBF	objective function
SOGA	single-objective genetic algorithm

REFERENCES

[1] Heinz-Adolf Schreiber, Wolfgang Steinert, and Bernhard Kuesters. Effects of reynolds number and freestream turbulence on boundary layer transition in a compressor cascade. *Journal of Turbomachinery*, 124(1):1–9, February 2000.

[2] Ulf Koeller. *Entwicklung einer fortschrittlichen Profilsystematik fuer stationaere Gasturbinenverdichter*. PhD thesis, Ruhr-Universität Bochum, DLR-Forschungsbericht 1999-20, 1998.

[3] Frank Sieverding, Beat Ribi, Michael Casey, and Michael Meyer. Design of industrial axial compressor blade sections for optimal range and performance. *Journal of Turbomachinery*, 122(2):323–331, April 2004.

[4] Brenda M. Kulfan and John E. Bussoletti. Fundamental parametric geometry representations for aircraft component shapes. *AIAA Paper 2006-6948*, pages 1–45, 2006.

[5] Hermann Schlichting and Erich Truckenbrodt. *Aerodynamics of the Airplane (Translated by H. J. Ramm)*. McGraw-Hill International Book Company, Berlin, Germany, 2. edition, 1979.

[6] Mark Drela and Harold Youngren. *A User's Guide to MISES 2.63*. MIT Aerospace Computational Design Laboratory, February 2008.

[7] M. B. Giles. Newton solution of steady two-dimensional transonic flow. *GTL Report No. 186*, 1985.

[8] M. Drela. Two-dimensional transonic aerodynamic design and analysis using the euler equations. *GTL Report No. 187*, 1986.

[9] B. J. Abu-Ghannam and R. Shaw. Natural transition of boundary layers–the effects of turbulence, pressure gradient, and flow history. *Journal of Mechanical Engineering Science*, 22(5):213–228, October 1980.

[10] Mark Drela. *MISES Implementation of Modified Abu-Ghannam / Shaw Transition Criterion (Second Revision)*. MIT Aero-Astro, 1998.

[11] Heinz-Adolf Schreiber, Wolfgang Steinert, Toyotaka Sonoda, and Toshiyuki Arima. Advanced high-turning compressor airfoils for low reynolds number condition - part II: Experimental and numerical analysis. *Journal of Turbomachinery*, 126(4):482–492, December 2004.

[12] Toyotaka Sonoda and Heinz-Adolf Schreiber. Aerodynamic characteristics of supercritical outlet guide vanes at low reynolds number conditions. *Journal of Turbomachinery*, 129(4):694–704, August 2007.

[13] Ernesto Benini and Andrea Toffolo. Development of high-performance airfoils for axial flow compressors using evolutionary computation. *Journal of Propulsion and Power*, 18(3):544–554, May 2002.

[14] U. Stark and H. Hoheisel. The combined effect of axial velocity density ratio and aspect ratio on compressor cascade performance. *Journal of Engineering for Power*, 103(1):247–255, January 1981.

[15] Udo Stark. Ebene Verdichtergitter in quasi zweidimensionaler Unterschallströmung. *VDI Forschungsheft 641/87*, pages pp. 247–255, 1987.

[16] B.M. Adams, L.E. Bauman, W.J. Bohnhoff, K.R. Dalbey, M.S. Ebeida, J.P. Eddy, M.S. Eldred, P.D. Hough, K.T. Hu, J.D. Jakeman, J.A. Stephens, L.P. Swiler, D.M. Vigil, and T.M. Wildey. *Dakota, A Multilevel Parallel Object-Oriented Framework for Design Optimization, Parameter Estimation, Uncertainty Quantification, and Sensitivity Analysis: Version 6.4 User's Manual*, Sandia Technical Report SAND2014-4633 edition, Updated May 9 2014.